PHYSICAL REVIEW B VOLUME 25, NUMBER 6 15 MARCH 1982

# Alloy broadening of impurity electronic spectra: One-dimensional tight-binding theory for a binary alloy

Charles W. Myles
*Department of Physics and Engineering Physics, Texas Tech University, Lubbock, Texas 79409*

John D. Dow
*Department of Physics and Materials Research Laboratory, University of Illinois at Urbana-Champaign, Urbana, Illinois 61801*

(Received 11 September 1981)

A quantitative theory of inhomogeneous alloy broadening of impurity spectral lines is developed for substitutional crystalline alloys, with the use of the embedded-cluster method. Model calculations are presented for a defect in a tight-binding, one-state-per-atom, one-dimensional binary-alloy crystal $A_xB_{1-x}$ with nearest-neighbor interactions. Among the interesting effects discussed are the splitting of the impurity spectral lines into components which can be identified with the near-neighbor environment of the impurity and the dependence of these lines on both the alloy composition $x$ and the $A$-$B$ atomic-energy difference.

## I. INTRODUCTION

In a disordered system, fluctuations of local potential energy in the neighborhood of an impurity can both inhomogeneously broaden the impurity spectral lines which lie within a band gap and also produce local environments which can immobilize and hold excitations for relatively long times as they hop from one impurity to another. A classic set of experiments by Wolford, Streetman, and Thompson[1] on the excitons bound to nitrogen impurities in $GaAs_{1-x}P_x$ has recently served to highlight the importance of this alloy-broadening effect on the luminescence spectra of semiconducting alloys. These workers demonstrated that a bound exciton hops from one nitrogen to another by resonant energy transfer until it reaches a trap. They also determined that the alloy fluctuations which broaden the nitrogen impurity line can greatly inhibit this exciton transport to traps. This effect can thus be thought of as analagous to a "self-trapping" of the exciton by the alloy fluctuations. Finally, Wolford, Streetman, and Thompson demonstrated that this alloy "self-trapping" can increase the luminescence efficiency of this important light-emitting diode material by reducing the exciton diffusion length, thereby preventing the exciton from reaching a nonradiative recombination center.

Wolford, Streetman, and Thompson were able to measure the alloy-broadened linewidth and line shape of the nitrogen luminescence line as a function of host-alloy composition $x$. Unfortunately, however, a satisfactory microscopic theory of this line shape does not, to our knowledge, exist.[2] The purpose of the present paper is to lay the foundation for such a theory and to develop a calculational method which will be practical for application to real alloys such as $GaAs_{1-x}P_x$. For simplicity and clarity of presentation, we consider here a model alloy system and treat the effects of alloy disorder on impurity spectra in a one-dimensional, one-band, nearest-neighbor, tight-binding binary alloy. This model contains all of the essential physical elements of alloy broadening without the complications of a realistic, three-dimensional, multiband, multineighbor model. The initial treatment of such a model thus has the advantage that it enables us to develop a calculational technique and to test it on a system which is simple enough that the essential physics are not obscured by mathematical and computational complexities. The technique developed here is based upon a generalization of the embedded-cluster method,[3-5] which was developed earlier for calculating alloy vibrational spectra. We shall show in subsequent work that the basic ideas presented here, with some modifications for $sp^3$ chemical bonding, can be applied successfully to the problem of luminescence line shapes in III-V alloys such as $GaAs_{1-x}P_x$.

This paper is organized as follows. In Sec. II, the model is discussed and the notation we use is established. The basic formalism we use is outlined in Sec. III, where we briefly review the

 

coherent potential approximation[6-10] (CPA) for the alloy host, and discuss the application of the embedded-cluster method to the treatment of the effects of alloy disorder on impurity spectra.[11] In Sec. IV, we present results, obtained by the embedded-cluster method,[3-5] for the alloy-broadened line shapes of two different impurities in this model alloy system. A brief comparison with other theoretical approaches is made in Sec. V, and in Sec VI we present a brief discussion and conclusions. An appendix contains a discussion of perturbation theory in powers of the minority composition.

## II. MODEL AND NOTATION

In this paper we consider a binary alloy $A_xB_{1-x}$ which serves as the host for an isolated impurity, $I$. Although we do all of our calculations for a one-dimensional, one-state-per-atom, nearest-neighbor tight-binding model alloy system, most of the formalism is applicable in a straightforward but tedious manner to three dimensions and to alloy systems with more realistic electronic structure. Furthermore, most equations in this paper are, with appropriate generalizations, valid in three dimensions.

The alloy-host one-electron Hamiltonian in the tight-binding approximation is

$$H_0=\sum_n |n\rangle E_n\langle n| \sum_{\substack{n,n' \\ n'\neq n}} |n\rangle t_{nn'}\langle n'| \ , \tag{1}$$

where $|n\rangle$ is an atomiclike orbital centered at the $n$th site. Here we consider diagonal disorder and nearest-neighbor interactions only; thus the on-site matrix element $E_n$ is a random variable taking on the values $E_A$ and $E_B$ with probabilities $x$ or $1-x$, respectively, and the transfer matrix element has the form

$$t_{nn'}=t(\delta_{n,n'-1}+\delta_{n,n'+1}) \ , \tag{2}$$

where the nearest-neighbor interaction energy $t$ is assumed to be the same for all nearest-neighbor pairs and independent of $x$.

The alloy Green's-function matrix is defined as

$$G_0=(E-H_0+i0)^{-1} \ , \tag{3}$$

where $E$ is an energy and $i0$ is a positive imaginary infinitesimal. The configuration-averaged alloy density of states is defined in the usual manner,[10]

$$D_0(E)=-\frac{1}{\pi N}\mathrm{Im}(\mathrm{Tr}\langle\langle G_0\rangle\rangle) \ , \tag{4}$$

where the trace runs over all sites of the crystal, $N$ is the total number of atoms, and the double angular brackets denote an average over all alloy configurations.

Inserted in the alloy host at the origin is a defect with on-site matrix elements $E_I$ and a nearest-neighbor transfer matrix element which we take to be $t$, the same as for the rest of the crystal. The Hamiltonian for the alloy in the presence of the defect is thus

$$H=H_0+U \ , \tag{5a}$$

where $U$ has the form

$$U=|0\rangle(E_I-E_0)\langle 0| \ . \tag{5b}$$

The Green's function for the alloy-impurity system is defined as

$$G=(E-H+i0)^{-1} \ , \tag{6}$$

From this function, the total density of states, as well as various local densities of states may be obtained in the standard way.[10] Of most interest in this paper is the configuration-averaged local density of states at the impurity site. For a given alloy configuration, the local density of states at the origin (impurity site) is

$$L_0(E)=-\frac{1}{\pi}\mathrm{Im}\langle 0|G|0\rangle \ , \tag{7a}$$

and its configuration average is therefore

$$l_0(E)=\langle\langle L_0(E)\rangle\rangle \ . \tag{7b}$$

In this paper, we seek this configuration-averaged density of states for energies $E$ in the band gap of the pure alloy, that is, where the density of states $D_0(E)$ of the alloy host vanishes.

## III. METHOD

We compute the density of states $l_0(E)$, Eq. (7), using the embedded-cluster method as developed by Gonis and Garland[3] and by the present authors.[4,5] The basic idea of this method, as used in this paper, is that the alloy host is treated by embedding a cluster in a self-consistent effective medium, described here by the coherent potential approximation (CPA).[6-10] We perform these calculations using a cluster of $N_c+1$ atoms, where $N_c$

is even, and the central atom of the cluster is the impurity responsible for the persistent impurity level. Every distinct configuration of the $N_c$ alloy constituent atoms which surround the impurity in the cluster leads to a different impurity energy level.[12] The levels associated with the various cluster configurations are the components of the alloy-broadened line shape.

For the model alloy considered here, both the CPA[6–10] and the embedded-cluster-method treatment[13] of the alloy host are discussed in detail elsewhere. However, it is useful, for reasons of completeness, to briefly summarize these methods here. Other workers[10,14–21] have developed self-consistent cluster theories (cluster CPA theories), which could, in principle, be applied to the problem of alloy broadening of impurity electronic spectra. However, these would be computationally more difficult to carry out than the present theory.

### A. Coherent potential approximation

In the single-site CPA treatment of the alloy host,[6–10] one seeks to approximate the random alloy by a translationally invariant effective medium which is described by the best quasieigenstates of the statistically averaged alloy. The effective-medium Green's function is thus defined as the configurations average of the alloy Green's function,

$$g_0=\langle\langle G_0\rangle\rangle \ . \tag{8}$$

In the CPA, this Green's function is assumed to satisfy

$$g_0=(E-\langle\langle H_0\rangle\rangle+i0)^{-1} \ , \tag{9}$$

where the configuration-averaged Hamiltonian is written in the single-site approximation as

$$\langle\langle H_0\rangle\rangle=\sum_n |n\rangle\sigma(E)\langle n|+\sum_{\substack{n,n'\\ n'\neq n}} |n\rangle t_{nn'}\langle n'| \ . \tag{10}$$

Here, $\sigma(E)$ is the (as yet undetermined) complex energy-dependent self-energy describing the single-site CPA medium. The effective medium described by this self-energy is determined by the requirement that its quasiparticles scatter the minimum amount, that is, that the single-site effective-medium transition matrix is zero when averaged over all possible alloy configurations. This leads to the condition

$$\langle\langle\tau_n\rangle\rangle=x\tau_A+(1-x)\tau_B=0 \ , \tag{11a}$$

where

$$\tau_{A(B)}=\{1-[E_{A(B)}-\sigma(E)]\langle n|g_0|n\rangle\}^{-1} \times[E_{A(B)}-\sigma(E)] \ , \tag{11b}$$

is the single-site transition matrix for an $A$ ($B$) site. Equations (11a) and (11b), when combined with the diagonal matrix elements of Eq. (9), yield a self-consistent equation for the self-energy $\sigma(E)$. As is shown elsewhere,[13] for the one-dimensional nearest-neighbor tight-binding model, this reduces to a cubic algebraic equation.

In order to solve Eq. (11) and obtain the self-energy, it is clearly necessary to express the Green's function $\langle n|g_0|n\rangle$ in terms of $\sigma(E)$. Also, for use in the embedded-cluster method discussed below, it will be useful to have a specific form for the general CPA Green's functions in the site representation, $\langle n|g_0|n'\rangle$. These functions may be easily obtained in the one-dimensional nearest-neighbor tight-binding model. In this case, they have the form[13]

$$\langle n|g_0|n'\rangle=\{\tilde{E}+[(\tilde{E})^2-1]^{1/2}\}^{|n-n'|} \times[(\tilde{E})^2-1]^{-1/2}/2|t| \ , \tag{12a}$$

where

$$\tilde{E}=[E-\sigma(E)]/2|t| \ . \tag{12b}$$

### B. Embedded-cluster method for calculation of impurity spectra

In the present theory of impurity spectra we treat the alloy host via the embedded-cluster method.[3–5] As applied here, an ensemble of $N_c+1$ atom clusters of different configurations is embedded in a CPA medium described by the Green's function $\langle n|g_0|n'\rangle$, Eq. (12); the medium is not altered to account for the effect of the impurity on it. Here, $N_c$ must be even and the central site of each cluster contains the impurity atom. The Green's function for the cluster with a specific configuration has the form shown in Eq. (6) and satisfies the Dyson equation

$$G=g_0+g_0VG \ , \tag{13}$$

where $V$ is a scattering potential which may be written

$$V=H-\langle\langle H_0\rangle\rangle=H_0-\langle\langle H_0\rangle\rangle+U \ , \tag{14}$$

for sites within the cluster and which vanishes outside of the cluster. The $(N_c+1)\times(N_c+1)$ matrix equation given by Eq. (13) may be solved numerically to yield

$$G=(1-g_0V)^{-1}g_0 \ . \tag{15}$$

The configuration-averaged local density of states at the impurity site may then be obtained by the use of Eq. (7).

The primary approximation in the application of the embedded-cluster method to the calculation of impurity spectra is thus that the Green's function given by Eq. (15) is, in fact, the Green's function for the random-alloy host in the presence of the impurity. If one takes the cluster size large enough and considers every possible configuration of alloy constituents for a cluster of $N_c$ atoms,[12] the configuration-averaged local environment seen by the impurity will approach that seen by an impurity in the random alloy. Results obtained by the use of this formalism on the model-alloy system considered here are discussed in the next section.

## IV. RESULTS

The use of the embedded-cluster formalism described in the last section for the calculation of the local state density $l_0(E)$ for energies in the band gap of the host alloy results in a spectrum which is a series of δ-function impurity lines, one for each distinct cluster configuration. Since δ functions are difficult to handle numerically, in practice the method we have used to obtain the function $l_0(E)$ is to find, for each configuration, the zero of the function $1/\langle 0\,|\,G\,|\,0\rangle$ which occurs in the band gap, where $G$ is given by Eq. (15). Then, for a given composition $x$ and cluster size $N_c$, the local state density may be represented as

$$l_0(E)=\sum_i P_i\delta(E-E_i) \ , \tag{16}$$

with the normalization condition $\sum_i P_i=1$. Here, $P_i$ is the probability of random occurrence of the $i$th cluster configuration, $E_i$ is the energy of the impurity in the $i$th configuration (obtained by finding the zero of the function $1/\langle 0\,|\,G\,|\,0\rangle$ for that configuration), and the sum goes over all possible configurations of the $N_c$ alloy constituent atoms in the cluster.[12]

Because of the form of the function $l_0(E)$, which will be referred to in what follows as the "line shape," it is useful to discuss the results for this function in terms of configuration-averaged moments of the spectrum. The configuration-averaged $n$th moment may be easily evaluated from Eq. (16) and has the form

$$L_n=\langle\langle E^n\rangle\rangle=\int_{-\infty}^{\infty}dE\,l_0(E)E^n \ , \tag{17a}$$

or

$$L_n=\langle\langle E^n\rangle\rangle\sum_i P_iE_i^n \ . \tag{17b}$$

If the impurity energy $E_i$ lies outside the band gap, the term for the $i$th configuration is not included in the sum. It is also often convenient to discuss the $n$th moment about the mean, which is defined as

$$M_n=\langle\langle(E-\langle\langle E\rangle\rangle)^n\rangle\rangle \ . \tag{18}$$

Of particular interest in the present paper are the first moment, or configuration-averaged energy, and the $n$th root of the $n$th moment about the mean for $n=2$, 3, and 4. For these latter quantities, we shall use the symbols

$$\Delta=[M_2]^{1/2}=[\langle\langle(E-L_1)^2\rangle\rangle]^{1/2}=(L_2-L_1^2)^{1/2} \ , \tag{19a}$$

$$\alpha=[M_3]^{1/3}=[\langle\langle(E-L_1)^3\rangle\rangle]^{1/3}=(L_3-3L_2+2L_1^3)^{1/3} \ , \tag{19b}$$

and

$$\beta=[M_4]^{1/4}=[\langle\langle(E-L_1)^4\rangle\rangle]^{1/4}=(L_4-4L_3L_1+6L_2L_1^2-3L_1^4)^{1/4} \ . \tag{19c}$$

The quantities Δ and $\alpha$ are usually referred to as the linewidth and skewness (or asymmetry), respectively.

Again because of the form of Eq. (16), it is sometimes useful to artificially broaden the δ-function peaks to enable one to "see" the line shape. For the cases discussed below we do this by convolving Eq. (16) with a Gaussian of width Γ. The results of this manipulation are

$$d(E)=\int_{-\infty}^{\infty}l_0(E')B(E-E')dE' \ , \tag{20a}$$

where the Gaussian broadening function is

$$B(E)=\frac{1}{\sqrt{2\pi}\,\Gamma}e^{-E^2/2\Gamma^2} \ . \tag{20b}$$

Thus, we have

$$d(E)=\frac{1}{\sqrt{2\pi}\Gamma}\sum_i P_i e^{-(E-E_i)^2/2\Gamma^2} \tag{20c}$$

### A. Results for the case $E_A=-E_B=3.0$, $t=1.0$, $E_I=0.0$, and $N_c=8$ (symmetric case)

These parameters correspond to the case of an alloy in the "persistence"[8] limit, that is with the band spectra of $A$ and $B$ nonoverlapping. In Fig. 1 we show the results in this case for the dependence of the first moment or configuration-averaged energy $L_1$ on the alloy composition $x$. The defect potential produces an impurity spectral line between the $A$ and $B$ bands. We focus our attention on this impurity line. The host energy bands are shaded and the band edges are the same as in the CPA. The solid line denotes the overall ("total") first moment $L_1$, which varies approximately linearly with alloy composition $x$. When viewed with finer resolution (see also Figs. 3 and 4), the impurity line has three distinct components, which are denoted in Fig. 1 as *BIB*, *AIB*, and *AIA*, and are associated with configurations in which the impurity atom $I$ is surrounded by two $B$ atoms, one $A$ atom and $B$ atom, and two $A$ atoms, respectively. With even finer resolution (see Fig. 4), these three-component spectra exhibit even further fine structure.

By keeping only configurations in the sum in Eq. (17b), which have a particular one of the three

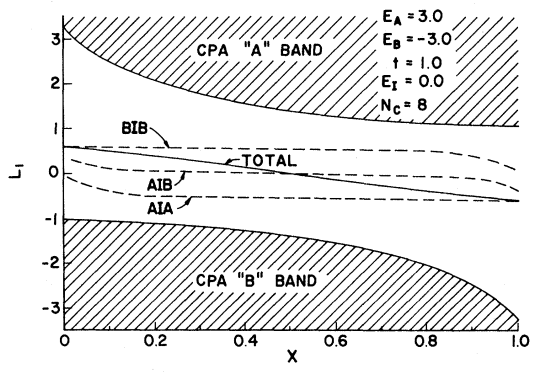


FIG. 1. First moment $L_1$ of the alloy-broadened line shape vs alloy composition $x$ for $A_xB_{1-x}$ in the symmetric case $E_A=-E_B=3.0$, $t=1.0$, $N_c=8$, and $E_I=0.0$. The solid line is the total contribution to $L_1$ and the dashed lines are from the components lying within the band gap associated with the impurity nearest-neighbor configurations *AIA*, *AIB*, and *BIB*.

impurity near-neighbor environments, and by appropriately renormalizing the probabilites, it is possible to compute the moments of these component lines. The dependences of the first moments on $x$ for these three lines are also shown in Fig. 1 (dashed lines), where the components are appropriately labeled. As may be seen from that figure, the component lines do not vary linearly with $x$, but are, in fact, except for large and small $x$, almost constant over most of the composition range. It is interesting to note that the *BIB* line, for the model parameters chosen, lies above the *AIA* line. This occurs because the adjacent $A$'s, being higher in energy than the impurity, repel the impurity level downward, while the $B$'s, being lower in energy, repel the level upward.

The present calculations have been performed in the range $0.01\leq x\leq 0.99$. However, they are expected to be most accurate in the range $1/N_c \leq x\leq 1-1/N_c$. Outside of this range, errors can be expected to occur. For practical reasons, we have not done any calculations for $N_c>8$. Thus, we expect the calculations in the range $0.125 \leq x\leq 0.875$ to be the most accurate. However, by doing an exact calculation for an isolated impurity in a pure $B$ or $A$ lattice, it is possible to extrapolate the present results to $x\rightarrow 0$ and $x\rightarrow 1$. We have done this for the case shown in Fig. 1 and in that figure the results of the embedded-cluster method have been joined smoothly to the exact isolated impurity results at $x=0$ for the "total" and *BIB* lines and at $x=1$ for the "total" and *AIA* lines. Similar extrapolation for *AIB* at $x=0$ and $x=1$, *BIB* at $x=1$, and *AIA* for $x=0$ would require the exact treatment of pairs and triplets of impurities.

In Fig. 2, the composition dependences of the linewidth $\Delta$, the skewness $\alpha$, and the fourth root of the fourth moment $\beta$ of the alloy-broadened line shape are shown for the same parameters as used in Fig. 1. Since the impurity in this case is chosen with an atomic energy halfway between the atomic energies of $A$ and $B$ ($E_A=-E_B=3.0$, $E_I=0.0$), the quantities $\Delta$ and $B$ (even roots of even moments about the mean) are symmetric about $x=0.5$, while the skewness $\alpha$ (odd root of an odd moment about the mean) is antisymmetric. It is clear from this figure that the line shape, even for this symmetric case, has significant third and fourth moments for most compositions. Thus, the overall line shape is not representable by a simple function and the usual moment expansions of impurity line shapes may be, at best, slowly convergent. Furthermore, the quantities $\Delta$, $\alpha$, and $\beta$ de-

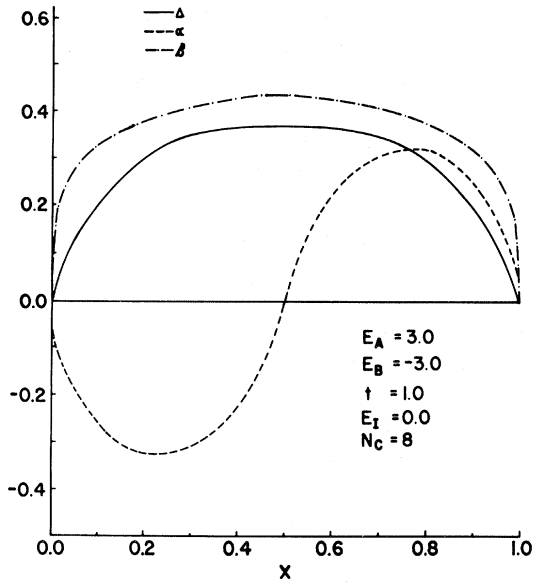


FIG. 2. Linewidth Δ (solid curve), skewness or asymmetry $\alpha$ (dashed curve), and fourth root of the fourth moment $\beta$ (dotted-dashed curve) of the alloy-broadened line shape as functions of alloy composition $x$ for the same parameters as used in Fig. 1.

viate considerably from the $[x(1-x)]^{1/n}$ composition dependence which is shown in the Appendix to be predicted for the $n$th root of the $n$th moment about the mean by a perturbation theory in powers of the minority concentration. For example, the linewidth Δ deviates by as much as 20% from its expected $[x(1-x)]^{1/2}$ dependence, even if one normalizes the perturbation and embedded-cluster method results at $x=0.5$ to ensure maximum agreement.[11] Furthermore, this deviation becomes larger as $n$ increases. This deviation is perhaps not too surprising, since such a perturbation theory is expected to be strictly valid only in the limits $x\to 0$ and $x\to 1$.

Because we have performed these moment calculations only for clusters as large as $N_c=8$, the embedded-cluster calculation results for Δ, $\alpha$, and $B$ are again expected to be most accurate in the range $0.125\leq x\leq 0.875$. However, at extremely small ($x\to 0$) and large ($x\to 1$) alloy compositions, the perturbation theory in the minority concentration discussed in the preceding paragraph is expected to be valid. Thus, in plotting Fig. 2, we have smoothly joined our embedded cluster results to the $[x(1-x)]^{1/n}$ dependence predicted by this perturbation theory.

We have also calculated the linewidths of the component spectra *BIB*, *AIB*, and *AIA* as functions

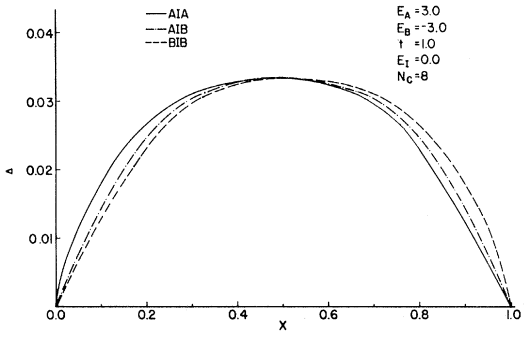


FIG. 3. Linewidths Δ for the component lines of the alloy-broadened line shape associated with the impurity nearest-neighbor environments *AIA* (solid curve), *BIB* (dashed curve), and *AIB* (dotted-dashed curve) as functions of alloy composition $x$ for the same parameters as used in Fig. 1.

of alloy composition for the same parameters as used in Figs. 1 and 2. In Fig. 3, we show the results of this calculation. As may be seen from that figure, the overall shape of these curves for line width versus $x$ is not very different from that of the overall linewidth shown in Fig. 2. However, their maximum values (at $x=0.5$) are about an order of magnitude smaller than the maximum value of the "total" linewidth. Furthermore, as is intuitively reasonable for this case where the atomic energies of $A$ and $B$ are symmetric about the impurity, the *AIB* linewidth is symmetric about $x=0.5$ while the *AIA* and *BIB* linewidths are slightly skewed towards small $x$ and large $x$, respectively. We have also computed the parameters $\alpha$ and $\beta$ for these component lines. These calculations show that both the shapes of these quantities as a function of $x$ and their relative magnitudes in comparison with the corresponding linewidths are very similar to those of their counterparts for the overall lines.

A final illustration of this case where the impurity atomic energy is halfway between those of $A$ and $B$ is shown in Fig. 4. That figure displays the Gaussian-broadened impurity line shapes, computed by the use of Eq. (20), for the alloy compositions $x=0.05$, 0.1, 0.3, and 0.5. In generating these curves the same parameters as for Figs. 1–3 were used and each line shape is shown for three different choices of the Gaussian width Γ. The narrowest peaks (spikes) shown in Fig. 4 (solid lines) correspond to $\Gamma=3\times 10^{-3}$, the next narrowest peaks (dashed lines) to $\Gamma=3\times 10^{-2}$ and the wide envelopes (dotted lines) to $\Gamma=3\times 10^{-1}$. It is clear from Fig. 4 that these predicted line shapes are rich in structure that would be missed by most

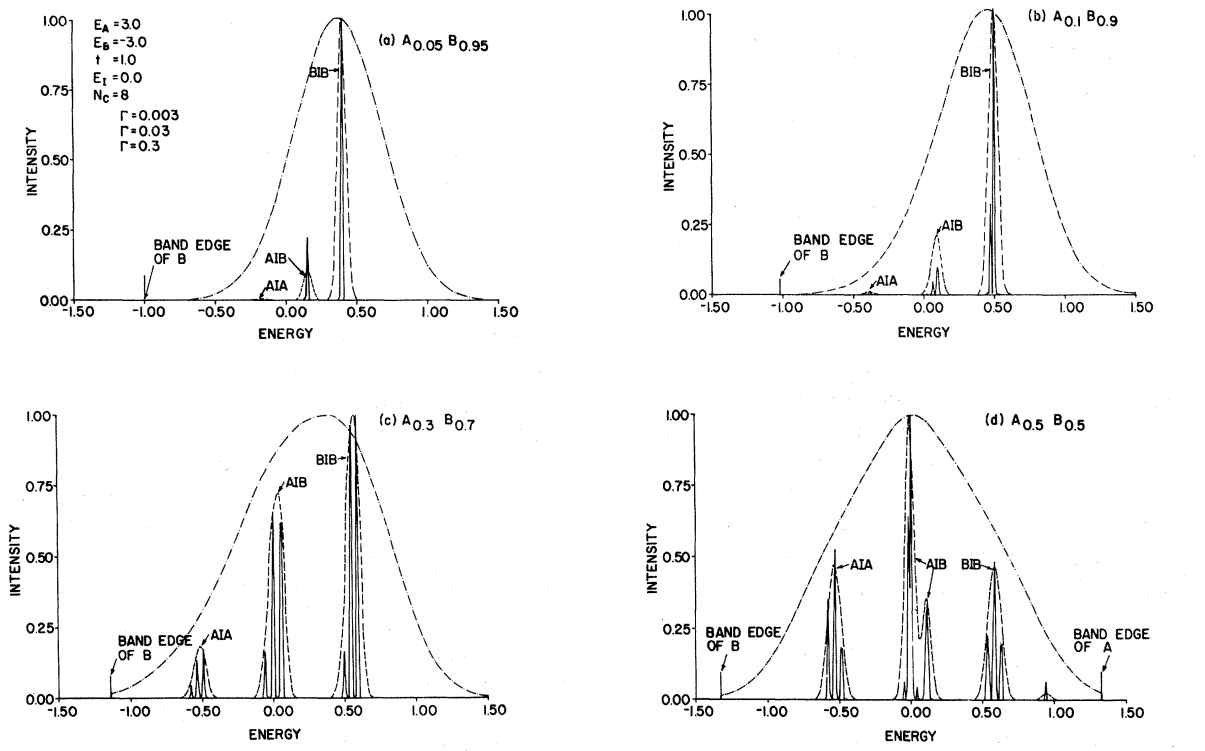


FIG. 4. Gaussian-broadened impurity line shape for the alloy $A_xB_{1-x}$ for the same parameters as used in Fig. 1. Three different Gaussian broadenings are displayed: $\Gamma = 3\times10^{-3}$ (solid curves), $\Gamma = 3\times10^{-2}$ (dashed curves), and $\Gamma = 3\times10^{-1}$ (dotted-dashed curves). (a) $x = 0.05$, (b) $x = 0.1$, (c) $x = 0.3$, and (d) $x = 0.5$. The line shapes for different $x$ are symmetric about $x = 0.5$, upon reflection through $E = 0.0$. Thus, only line shapes for $x \leq 0.5$ have been shown.

simple perturbation or moment expansion theories.

The finest resolution curves (solid lines) for the line shapes clearly show the existence of many impurity energy levels; each level corresponds to a different configuration of alloy constituents in the cluster (some of these are degenerate or almost degenerate). It is also clear from Fig. 4 that, in confirmation of the moment information shown in Figs. 1 and 3, these narrow peaks form three distinct groups, which may be identified with cluster configurations containing the *AIA*, *BIB*, and *AIB* impurity nearest-neighbor configurations. These groups of peaks are labeled corresponding to these identifications. The relative heights of the peaks and the shapes of the broader curves are determined by the relative probabilities of the occurrence of the cluster configuration which gives rise to a particular level for a fixed composition $x$.[12] The vertical scale in Fig. 4 is arbitrary; the curves are normalized so that the highest peak height is always unity.

The curves with intermediate resolution (dashed lines) in Fig. 4. tend to smooth all but the gross features of the energy-level structure, but still clearly reflect the fact that the spectrum has three main components. The curves in Fig. 4 with largest broadening (dotted-dashed lines) each show only an almost featureless Gaussian-like bump which forms an envelope over the curves for the smaller broadenings.

The line shapes for different $x$ are symmetric about $x = 0.5$; that is, the $x = 0.5$ line shape is symmetric in energy about $E = 0$ and the line shapes for $x$ on either side of $x = 0.5$ are mirror images of one another. Thus, only line shapes for $x \leq 0.5$ have been shown in Fig. 4. For example, the $x = 0.3$ line shape would be identical to the $x = 0.7$ line shape if the latter were plotted versus $-E$ instead of $E$. This behavior is to be expected, because the impurity level is halfway in energy between those of the two alloy constituents.

In a real alloy, the actual impurity line shape could range anywhere from those shown in Fig. 4 for the finest resolution to those shown for the broadest resolution, depending on the physical mechanism responsible for this level broadening.

### B. Results for the cases $E_A=-E_B=3.0$, $t=1.0$, $E_I=1.0$, and $N_0=8$ (asymmetric case)

We have also calculated the moments and line shapes of the alloy-broadened impurity spectrum in the case where all parameters are the same as in Figs. 1–4, except that the impurity energy is moved upward to $E_I=1.0$, destroying the symmetry of the $A$ and $B$ host atomic energies about the impurity atomic energy.

In Fig. 5 we display the dependence of the configuration-averaged energy $L_1$ on alloy composition for this case. The solid line denotes the overall ("total") first moment, which again varies almost linearly with $x$. As in the previous case, the impurity line, when viewed with finer resolution, is seen to have three distinct components which may be identified with the impurity nearest-neighbor environments *BIB*, *AIB*, and *AIA*. The composition dependence of the first moments of these component lines is also shown in Fig. 5 (dashed lines), where they are appropriately labeled. As may be seen from this figure, these component lines do not vary linearly with $x$. Furthermore, unlike the corresponding lines for the symmetric case (Fig. 1), which deviate from constants only for large and small $x$, these component lines show a significant amount of bending as a function of $x$ for all compositions. It is also interesting to note that, for this case, the center of the *BIB* line approaches the $A$-band edge for $x \gtrsim 0.7$.

The results of the embedded-cluster-method calculations for this asymmetric case are again expected to be most accurate in the composition range $0.125 \leq x \leq 0.875$, since they were done for $N_c=8$. Thus, outside of this range they have, where possible, been smoothly joined in Fig. 5 to the exact results at $x \to 0$ and $x \to 1$ for a single impurity in a pure $B$ or $A$ lattice.

The composition dependences of the linewidth $\Delta$, the skewness $\alpha$, and the quantity $\beta$, of the alloy-broadened line shape are shown in Fig. 6 for the same parameters as were used in Fig. 5. The interesting feature of this case is that, since $E_A$ and $E_B$ are not symmetric about the impurity atomic energy $E_I$, the quantities $\Delta$, $\alpha$, and $\beta$ all show a marked assymmetry about $x=0.5$. In fact, all three parameters are larger in magnitude for $x<0.5$ than they are for the "mirror" compositions at $x>0.5$. The primary reason for this is that as $x$ increases (for $x>0.5$), more and more cluster configurations with the *BIB*-impurity nearest-neighbor configuration produce levels that are resonant with the $A$ band and are thus excluded from the sum in Eq. (17b). Thus, for $x>0.5$, the moments are depleted compared to those for $x<0.5$ and they are therefore skewed towards small $x$ when plotted as a function of composition. This fact also helps explain why the center of the *BIB* line (Fig. 5) approaches the $A$-band edge at

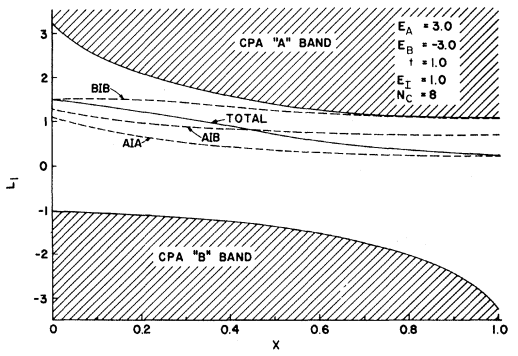


FIG. 5. First moment $L_1$ of the alloy-broadened line shape vs alloy composition $x$ for $A_xB_{1-x}$ in the asymmetric case $E_A=-E_B=3.0$, $t=1.0$, $N_C=8$, and $E_I=1.0$. The solid line is the total contribution to $L_1$ and the dashed lines are from the components lying within the band gap associated with the impurity nearest-neighbor configurations *AIA*, *AIB*, and *BIB*.

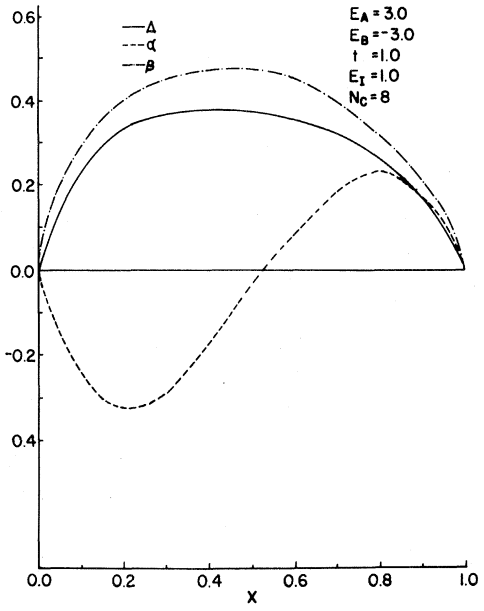


FIG. 6. Linewidth $\Delta$ (solid curve), skewness or asymmetry $\alpha$ (dashed curve), and fourth root of the fourth moment $\beta$ (dotted-dashed curve) of the alloy-broadened line shape as functions of alloy composition $x$ for the same parameter as used in Fig. 5.

large $x$.

It is clear from Fig. 6 that the linewidth $\Delta$, the skewness $\alpha$, and the fourth root of the fourth moment $\beta$, all deviate significantly from the $[x(1-x)]^{1/n}$ composition dependence shown in the Appendix to come from simple perturbation theory. This deviation is even more striking in the asymmetric case than in the previously discussed symmetric case, since the moments about the mean are not symmetric about $x=0.5$, as an extrapolation of this simple pertubation theory away from $x\rightarrow 0$ and $x\rightarrow 1$ predicts. However, such a perturbation theory is still expected to be accurate as $x\rightarrow 0$ or $x\rightarrow 1$, even in this asymmetric case. For this reason, and because the embedded-cluster-method calculations are again inaccurate in those limits, we have joined the embedded-cluster results shown in Fig. 6 smoothly to the perturbation-theory results at large and small $x$.

For the same case, we have also calculated the composition dependence of the linewidths of the component spectra *BIB*, *AIB*, and *AIA*. In Fig. 7, we show the results of this calculation. As may be seen from that figure, the linewidths of the *AIA* and *AIB* components are, unlike the overall linewidth (Fig. 6), almost symmetric about $x=0.5$. In contrast, however, the *BIB* linewidth is extremely asymmetric about $x=0.5$ and is, in fact, essentially completely depleted for $x\gtrsim 0.7$. The reason for this is the same as the above discussed reason for the asymmetry of the overall linewidth. Indeed, Fig. 7 shows that the asymmetry of the total linewidth is due, in large measure, to the large asymmetry of the *BIB* linewidth.

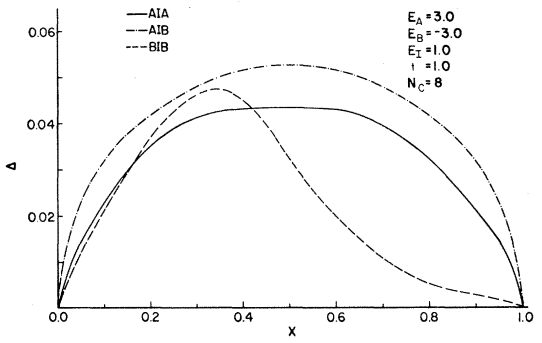


FIG. 7. Linewidths $\Delta$ for the component lines of the alloy-broadened line shape associated with the impurity nearest-neighbor environments *AIA* (solid curve), *BIB* (dashed curve), and *AIB* (dotted-dashed curve) as functions of alloy composition $x$ for the same parameters as used in Fig. 5.

In Fig. 8 we display the Gaussian-broadened impurity line shapes, computed by the use of Eq. (20) for the same parameters as used in Figs. 5–7. In that figure the line shapes for $x=0.05$, 0.1, 0.3, 0.5, 0.7, 0.9, and 0.95 are displayed, each with three different Gaussian broadenings, $\Gamma=3\times 10^{-3}$, $3\times 10^{-2}$, and $3\times 10^{-1}$. As in the symmetric case, the line shapes are very rich in structure and show many features which are unobtainable by the use of simple moment-expansion or perturbation theories.

The most interesting features of this case are again a direct result of the asymmetry of the impurity atomic energy with respect to the atomic energies of $A$ and $B$. This asymmetry manifests itself in at least two ways. The first and most prominent of these is the lack of symmetry of the line shapes about $x=0.5$. The second is a lack of symmetry about $E=0$, as is illustrated vividly by the very asymmetric $x=0.5$ line shape [Fig. 8(d)], which should be contrasted with the line shape symmetric about $E=0$ obtained for the $E_I=0$ case [Fig. 4(d)]. A large portion of this lack of symmetry is due to the fact that, as discussed above, the *BIB* component of the line shape becomes partially "autoionized" for $x\gtrsim 0.5$, having some subcomponents above the $A$-band edge.

The finest resolution curves in Fig. 8 (solid lines) again show clearly the existence of many energy levels corresponding to the many possible cluster configurations for $N_c=8$. Again, the subcomponent groups *BIB*, *AIB*, and *AIA* can be clearly distinguished in the figures, although as the *BIB* configurations begin to produce levels above the $A$-band edge for $x>0.5$, the *BIB* subcomponents below the band edge become spread out and overlap the *AIB* lines. These groups of peaks are labeled in the figure corresponding to the appropriate impurity nearest-neighbor configurations. The relative heights of the peaks and the shapes of the broader curves are again determined by the probabilities of occurrence of the particular configurations that give rise to them.

The line-shape curves with intermediate (dashed lines) and large (dotted-dashed lines) broadenings shown in Fig. 8 wash out most and all, respectively, of the fine structure shown by the narrow broadening. The curves with intermediate broadening do, however, still show the three distinct components. However, those with the largest broadening each show an almost featureless but asymmetric bump.

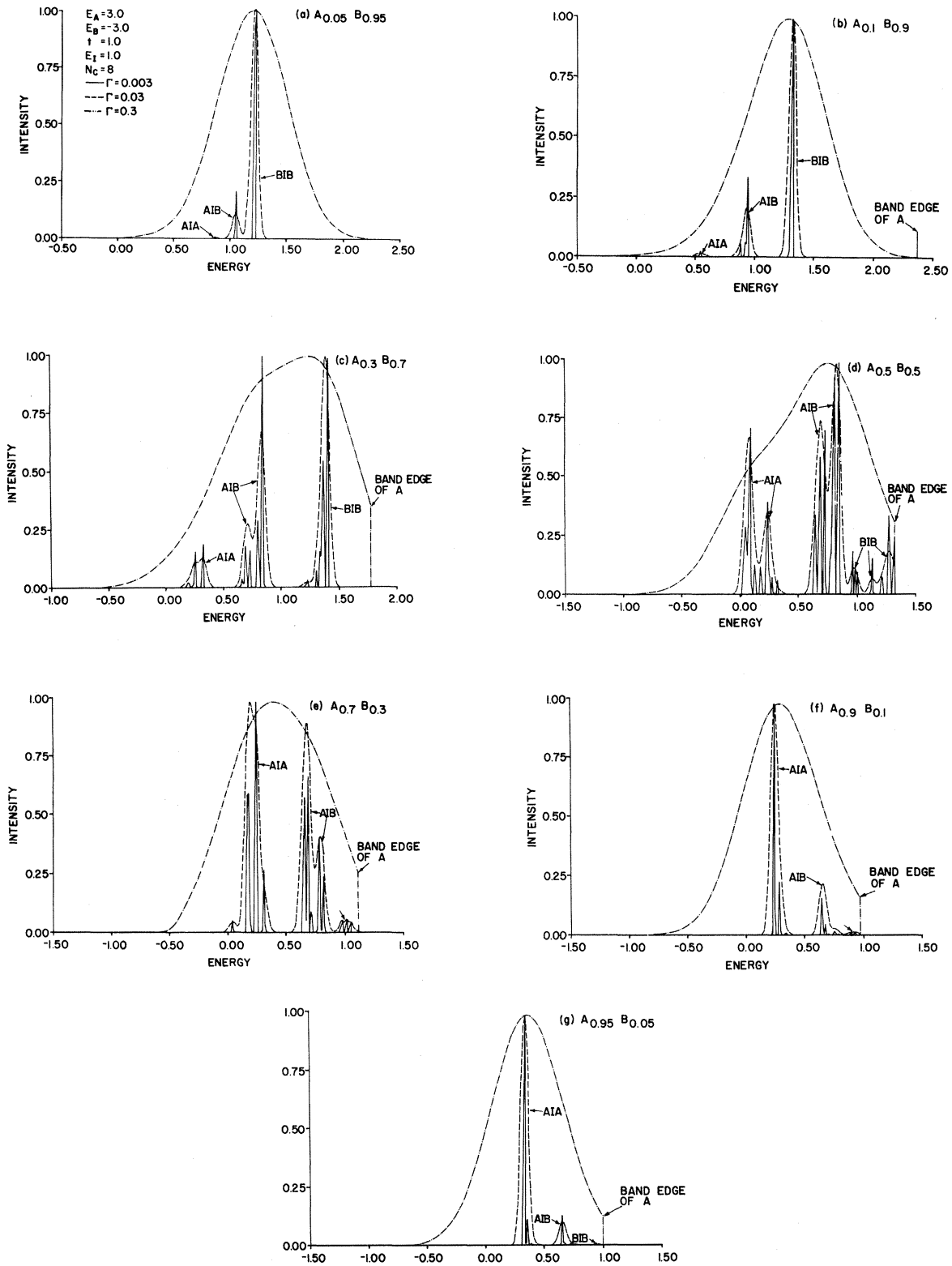


FIG. 8. Gaussian-broadened impurity line shapes for the alloy $A_xB_{1-x}$ for the same parameters as used in Fig. 5. Three different Gaussian broadenings are displayed: $\Gamma=3\times10^{-3}$ (solid curves), $\Gamma=3\times10^{-2}$ (dashed curves), and $\Gamma=3\times10^{-1}$ (dotted-dashed curves). (a) $x=0.05$, (b) $x=0.1$, (c) $x=0.3$, (d) $x=0.5$, (e) $x=0.7$, (f) $x=0.9$, and (g) $x=0.95$.

### C. Dependence on cluster size $N_c$

We have repeated some of the calculations discussed above for clusters of size $N_c=4$ and $N_c=6$. In general, we find a substantial difference between the $N_c=4$ and $N_c=6$ line-shape results, and only minor differences between the $N_c=6$ and $N_c=8$ results. Thus, it appears that the dependence of the major alloy-broadening effects on cluster size has saturated in one dimension at $N_c=8$. This is consistent with all of the results presented above, which show that the main effects are due to the nearest neighbors of the impurity and that second and more distant neighbors make only minor contributions to the alloy-broadened line shape. A typical result for the dependence of the alloy broadening on cluster size is shown in Fig. 9, where we show the linewidth $\Delta$ as a function of composition $x$ for the case $E_A=-E_B=3.0$, $t=1.0$, $E_I=0.0$, and for $N_c=4$ (dashed curve) and 8 (solid curve). The $N_c=6$ results show no major differences for $N_c=8$ and are indistinguishable on the scale of the figure from the latter results for most values of $x$.

### D. Dependence on the $A$-$B$ atomic energy difference

For some purposes it might be useful to study the effect on the alloy-broadened impurity line shape of changing the $A$-$B$ atomic energy difference. To this end, we have calculated the linewidth $\Delta$ as a function of the atomic difference $\delta \equiv E_A - E_B$ for a fixed alloy composition $x$. In Fig. 10 we display the results of this calculation for the symmetric case $E_A=-E_B$, $t=1.0$, $E_I=0.0$, $x=0.5$ and $N_c=8$.

For values of the energy difference $\delta$ smaller than are shown in the figure ($\delta<3$), the spectra cease to be "persistent"[8] and the energy gap in the alloy (in the CPA) closes up, causing the impurity line to become amalgamated[8] with and resonant with the alloy-host band spectra. This is the "amalgamation" limit of Onodera and Toyozawa,[8] and occurs when the band width becomes comparable with $\delta$. As $\delta$ increases above 3.0, the gap opens up and the linewidth becomes larger with increasing $\delta$; this is the limit in which the spectral components of $A$ and $B$ persist. This increase in linewidth with increasing $\delta$ can be qualitatively understood by noting that as $\delta$ increases, the impurity sees an increasingly larger fluctuation in potential difference between the $A$ and $B$ atoms. As this fluctuation increases, the linewidth of the configuration-averaged impurity line would be expected to increase. However as the $A$-$B$ energy difference becomes very large ($\delta=13$) the linewidth decreases and saturates as a function of $\delta$.

## V. COMPARISON WITH OTHER THEORETICAL APPROACHES

The present approach treats a cluster of $N_c+1$ atoms exactly, within the approximation that the cluster boundary conditions are specified by the CPA medium. Thus, insofar as the effects of the effective medium on the alloy-broadened impurity line shape can be neglected, this theory is an exact treatment of alloy broadening for an $N_c+1$ atom

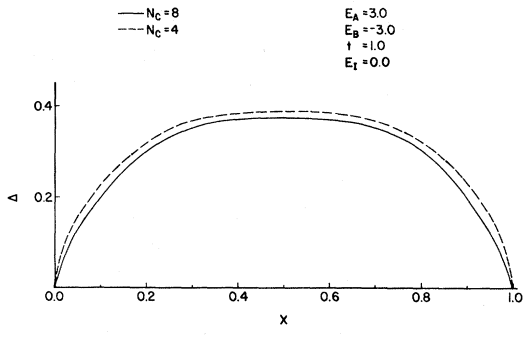


FIG. 9. Linewidth $\Delta$ of the alloy-broadened impurity line shape as a function of alloy composition $x$ in the symmetric case $E_A=-E_B=3.0$, $t=1.0$, and $E_I=0.0$, for two different cluster sizes: $N_c=8$ (solid curve) and $N_c=4$ (dashed curve).

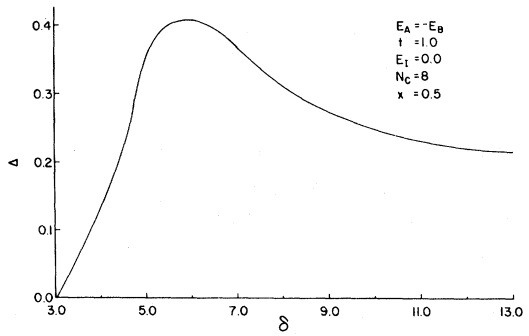


FIG. 10. Linewidth $\Delta$ of the alloy-broadened impurity line shape as a function of $\delta=E_A-E_B$ in the symmetric case $E_A=-E_B$, $t=1.0$, $E_I=0.0$, $N_c=8$, and $x=0.5$.

cluster. For $N_c$ large enough and for the short-ranged interactions considered here, the effects of the medium on the impurity energy levels should be minimal. Furthermore, our studies of the linewidth as a function of $N_c$ have shown that there is little change from $N_c=6$ to $N_c=8$. Thus, the present theory, although somewhat tedious, does produce an adequate alloy-broadened line shape, within these limitations. This is to be contrasted with other approaches which may fail in certain cases, even for a Hamiltonian of the simple form considered here.

For example, a perturbation expansion of the alloy line shape in powers of the minority constituent concentration ($x$ or $1-x$) is likely to be unreliable and, at best, slowly convergent in the alloy regime $0.05<x<0.95$. For the parameters chosen in Figs. 1—10 and for most alloy compositions $x$, the $n$th moments about the mean $M_n$ deviate significantly from the $x(1-x)$ dependence which is shown in the Appendix to result, in lowest order, from such a perturbation-theory expansion. In fact, except for the case of the "symmetric" ($E_I=0.0$) impurity, these moments are not even symmetric about $x=0.5$, as extrapolation of this simple perturbation theory away from $x\rightarrow 0$ and $x\rightarrow 1$ would predict. Furthermore, the electronic spectra in alloys are nonanalytic functions of the composition,[22] so that there is some question as to whether such a perturbation theory even converges to a physically meaningful limit.

As another possible approach to the theory of alloy broadening, one might develop a perturbation expansion in powers of the defect-host potential difference $U$. Such a theory can likewise become unreliable (and in fact divergent) because of strong mixing between the impurity level and the continuum, especially if some of the components of the alloy-broadened impurity line lie near a band edge or are resonant with a band continuum. Thus, a perturbation theory in the defect-host potential difference should be avoided when the impurity level lies near a band edge.

The impurity lines shown in Figs. 1—10 are often considerably asymmetric and have significant third, fourth, and higher moments. Thus, the description of the alloy-broadened line shape by a simple moment expansion is probably not possible. Since the usual moment theories of impurity line shapes[23] usually only keep the first few moments and furthermore usually assume a simple functional form for the line shape, such a theory would at best be slowly convergent and require many moments and at worst give an erroneous description of the impurity line shape.

The importance of compositional fluctuations in determining the alloy-broadened line shape is highlighted by the fact that the wings of the broadened impurity line are dominated by lines corresponding to significant fluctuations of the local environment from the average. For example, the particular cluster configuration *AAAIAAA* is certainly atypical for the alloy $A_{0.1}B_{0.9}$, but nevertheless contributes significantly to the line shape in this case. Thus, in our calculations we have had to consider *all* possible configurations of a small cluster, even the atypical ones, weighting each configuration by its probability of occurence for a particular composition $x$.[12] This contrasts with our earlier work on the alloy density of states, where we considered only cluster configurations with the average alloy composition.[4,5]

The fact that compositional fluctuations are important in determining the alloy-broadened impurity line shape means that the exact numerical determination of the impurity local-state density for 20 000-atom or larger chains using, for example, the negative-eigenvalue theorem method,[24—26] will not produce the correct alloy-broadened line shape either. In order to obtain the spectrum of isolated defects in such a chain, one must keep the defect concentration will below $\frac{1}{2}\%$ or $\sim 100$ atoms. However, we find that the number of local environments contributing significantly to the wings of the alloy-broadened line is also of the order of 100.[12] Thus, the number of defect atoms one would use with this method is too few to obtain a statistically complete and representative sampling of the possible impurity environments.

A multisite self-consistent cluster-CPA theory[14—21] would provide an approach to alloy-broadening theory that would be superior to the present theory. However, the computational labor involved would likely be enormous and perhaps prohibitive: The self-energy for every site of every cluster would have to be determined self-consistently. Less ambitious, non-self-consistent theories, such as a theory based on clusters embedded in an average $t$-matrix approximation medium[10,27] are computationally more tractable than the present approach, but less reliable.

The present theoretical approach, of treating the host as a self-consistent single-site-CPA, translationally invariant medium, and then (non-self-consistently) embedding in it clusters of moderate size offers a good balance between the need for

theoretical accuracy on the one hand and computational tractability on the other.

## VI. SUMMARY AND CONCLUSIONS

We have presented a general technique for calculating the effects of local environment on the spectra of impurities in alloys. To develop this technique and test the method, we have applied it here to a simple model binary-alloy system where the electrons are treated in the nearest-neighbor tight-binding approximation. By embedding an ensemble of clusters containing $N_c+1$ atoms in a CPA medium and letting the impurity be the central atom of these clusters, we have shown that one can calculate the alloy-broadened line shape of the impurity. Although the model chosen here is a simple one, the method does produce accurate alloy-broadened line shapes and shows promise for application to impurity spectra in real alloy systems.

The primary deficiency of the method, as presented here, is that it is not self-consistent. However, by introducing self-consistency as is done in the cluster-CPA theories,[14–21] this deficiency can be remedied—at some computational cost. As a rule, the primary effect of including self-consistency is to shift the band edges and impurity lines slightly, without greatly altering the qualitative physics.[14–21]

The general conclusions of this work are the following: (i) the nearest-neighbor environment of the impurity greatly affects persistent impurity lines and can either broaden or split those lines, (ii) second and third neighbors contribute significantly, often asymmetrically broadening the impurity lines, and (iii) the present method approach, although somewhat tedious, will generally produce an adequate alloy-broadened line shape, even when other methods fail. In future papers, the present method will be modified to account for $sp^3$ bonding and will be applied to real III-V semiconduting alloys.

## ACKNOWLEDGMENTS

One of the authors (C.W.M.) gratefully acknowledges the support of grants from the National Science Foundation (No. ECS-8020322), the Robert A. Welch Foundation (No. D-796), and the Research Corporation, each of which have supported this research at various stages; and thanks Texas Tech University for a grant of computer time to perform these calculations. The other author (J.D.D.) thanks the U.S. Office of Naval Research for their continuing support of this work (Contract No. N00014-77-C-0537). We are especially grateful to D. J. Wolford and B. G. Streetman, whose many conversations stimulated us to do this work and to O. F. Sankey who made many valuable suggestions during the early stages of the work.

## APPENDIX: PERTURBATION THEORY IN POWERS OF THE MINORITY COMPOSITION

One possible theory of alloy broadening of impurity spectra is a perturbation theory in the alloy minority composition. The following is a discussion of such a theory, along lines first suggested by Sankey.[28] This theory does, however, assume that (as is found in our theory) there are three distinct components of the alloy-broadened line shape characterized by the three possible nearest-neighbor environments and denoted as *BIB*, *AIB*, and *AIA*.

As in the text, we consider an alloy $A_xB_{1-x}$ in the "persistence"[8] limit and consider only impurity potentials $U$ which produce energy levels in the band gap of the alloy. Let the band-gap energies which result from the impurity nearest-neighbor environments *BIB*, *AIB* ($\equiv$*BIA*), and *AIA*, be denoted, respectively, as $\epsilon_1$, $\epsilon_0$, and $\epsilon_{-1}$. The probabilities of occurence of these three environments are $P_1=x^2$, $P_0=2x(1-x)$, and $P_{-1}=(1-x)^2$, respectively. For the following rough perturbation-theory calculation we assume that the parameters $\epsilon_1$, $\epsilon_0$, and $\epsilon_{-1}$ are independent of $x$.

Let $x$ be the alloy minority composition. Under the above assumptions, the $n$th moment of the overall ("total") impurity line is easily calculated from Eq. (17b) and has the form

$$L_n=\langle\langle E^n\rangle\rangle=\sum_n P_i E_i^n$$
$$=x^2\epsilon_1^n+2x(1-x)\epsilon_0^n+(1-x)^2\epsilon_{-1}^n . \quad \text{(A1)}$$

If only lowest-order terms in $x$ are kept, this becomes

$$L_n\cong 2x\epsilon_0^n+(1-2x)\epsilon_{-1}^n . \quad \text{(A2)}$$

The $n$th moment about the mean is calculated from Eq. (18) and is

$$M_n=\langle\langle(E-L_1)^n\rangle\rangle$$
$$=\left\langle\left\langle\sum_{i=0}^{n}\begin{bmatrix}n\\i\end{bmatrix}(-1)^{n-i}E^iL_1^{n-i}\right\rangle\right\rangle , \quad \text{(A3)}$$

where the standard binomial expansion has been used in the second step in Eq. (A3). Noting the definition of the $n$th moment $L_n$ and the properties of the configuration average, we may rewrite Eq. (A4) as

$$M_n=\sum_{i=0}^{n}\begin{bmatrix}n\\i\end{bmatrix}(-1)^{n-i}\langle\langle E^i\rangle\rangle L_i^{n-i}$$
$$=\sum_{i=0}^{n}\begin{bmatrix}n\\i\end{bmatrix}(-1)^{n-i}L_iL_1^{n-i}\ . \qquad \text{(A4)}$$

The substitution of Eq. (A2) into Eq. (A4) leads to

$$M_n=\sum_{i=0}^{n}\begin{bmatrix}n\\i\end{bmatrix}(-1)^{n-i}$$
$$\times[2x\epsilon_0^i+(1-2x)\epsilon_{-1}^i]$$
$$\times[2x\epsilon_0+(1-2x)\epsilon_{-1}]^{n-i}\ . \qquad \text{(A5)}$$

It is easily shown that, to lowest order in $x$, this has the form

$$M_n=2x(\epsilon_0-\epsilon_{-1})^n\ . \qquad \text{(A6)}$$

Thus, to lowest order in $x$, the $n$th moment of the impurity spectral line about the mean is linear in $x$ for all $n$. The $n$th root of the $n$th moment about the mean is

$$\Delta_n=(M_n)^{1/n}=(2x)^{1/n}\,|\,\epsilon_0-\epsilon_{-1}\,|\ . \qquad \text{(A7)}$$

and varies as $(x)^{1/n}$ for all $n$.

If, by contrast, we were to consider $1-x$ as the alloy minority composition and develop a perturbation theory in terms of this parameter, all of the above manipulations would carry through with the replacements $x\rightarrow 1-x$, $\epsilon_1\rightarrow\epsilon_{-1}$, and $\epsilon_{-1}\rightarrow\epsilon_1$. Thus, we would find in this case, to lowest order in $1-x$,

$$M_n=2(1-x)(\epsilon_0-\epsilon_1)^n\ , \qquad \text{(A8)}$$

and

$$\Delta_n=[2(1-x)]^{1/n}\,|\,\epsilon_0-\epsilon_1\,|\ . \qquad \text{(A9)}$$

Physically, it is reasonable that to lowest order these moments should be symmetric about $x=0.5$. This argument, combined with the above mathematical manipulations thus clearly leads to

$$M_n\propto x(1-x) \qquad \text{(A10)}$$

and

$$\Delta_n\propto[x(1-x)]^{1/n}\ . \qquad \text{(A11)}$$

In conclusion, it is perhaps worth noting that all of the above arguments will hold as well for the moments of the component lines *AIA*, *AIB*, and *BIB*, if one considers them each to be split into three groups corresponding to the possible second-nearest-neighbor environments.


[1]D. J. Wolford, B. G. Streetman, and J. Thompson, J. Phy. Soc. Jpn. 49, Suppl. A, 232 (1980).

[2]A number of partially phenomenological theories have been proposed. See, for example, H. Mariette, J. Chevallier, and P. Leroux-Hugon, Phys. Rev. B 21, 5706 (1980), and references therein.

[3]A. Gonis and J. W. Garland, Phys. Rev. B 16, 2424 (1977).

[4]C. W. Myles and J. D. Dow, Phys. Rev. B 19, 4439 (1979).

[5]C. W. Myles and J. D. Dow, Phys. Rev. Lett. 42, 254 (1979).

[6]P. Soven, Phys. Rev. 156, 809 (1967).

[7]D. W. Taylor, Phys. Rev. 156, 1017 (1967).

[8]Y. Onodera and Y. Toyozawa, J. Phys. Soc. Jpn. 24, 341 (1968).

[9]B. Velicky, S. Kirkpatrick, and H. Ehrenreich, Phys. Rev. 175, 747 (1968).

[10]Various analytic and quasianalytic approaches to the solution of the alloy problem, including the CPA and various cluster generalizations, are discussed in the article by R. J. Elliot, J. A. Krumhansl, and P. L. Leath, Rev. Mod. Phys. 46, 465 (1974), and references therein.

[11]C. W. Myles, J. D. Dow, and O. F. Sankey, Phys. Rev. B 24, 1137 (1981).

[12]For a given alloy composition $x$ and a cluster containing $N_c$ atoms with $N_A$ $A$ atoms and $N_B$ $B$ atoms ($N_A+N_B=N_c$), the number of configurations is

$$\begin{bmatrix}N_c\\N_A\end{bmatrix}=\frac{N_c!}{N_A!N_B!}\ ,$$

and a given configuration occurs with probability $p=x^{N_A}(1-x)^{N_B}$. Of course, not all cluster configurations are physically distinct.

[13]C. W. Myles (unpublished).

[14]W. H. Butler, Phys. Rev. B 10, 4499 (1973).

[15]R. L. Jacobs, J. Phys. F 3, 933 (1974); 4, 1351 (1974).
[16]N. Zaman and R. L. Jacobs, J. Phys. F 5, 1677 (1975).
[17]F. Brouers, M. Cyrot, and F. Cyrot-Lackmann, Phys. Rev. B 7, 4370 (1973).
[18]F. Brouers and F. Ducastelle, J. Phys. F 5, 45 (1975).
[19]F. Ducastelle, J. Phys. F 2, 468 (1972).
[20]W. H. Butler and B. G. Nickel, Phys. Rev. Lett. 30, 373 (1973).
[21]See also Refs. 9–27 in Ref. 4.
[22]I. M. Lifshitz, Adv. Phys. 13, 483 (1964).
[23]J. C. Phillips, Phys. Rev. 104, 1263 (1956).
[24]P. Dean, Rev. Mod. Phys. 44, 127 (1972), and references therein.
[25]D. N. Payton and W. M. Visscher, Phys. Rev. 154, 802 (1967); 154, 1032 (1967); 175, 1201 (1968).
[26]M. J. O'Hara, C. W. Myles, J. D. Dow, and R. D. Painter, J. Phys. Chem. Solids 42, 1043 (1981).
[27]P. L. Leath and B. Goodman, Phys. Rev. 181, 1062 (1969).
[28]O. F. Sankey (private communication).